

Supporting Information

Nanoporous Poly(3-hexylthiophene) Thin Film Structures from Self-Organization of a Tunable Molecular Bottlebrush Scaffold

Suk-kyun Ahn,^{*,a,e} Jan-Michael Carrillo,^{a,b} Jong K. Keum,^{a,c} Jihua Chen,^a David Uhrig,^a Bradley S. Lokitz,^a Bobby G. Sumpter,^{a,b} S. Michael Kilbey II^{*,d}

^aCenter for Nanophase Materials Sciences, ^bComputer Science and Mathematics Division,

^cSpallation Neutron Source, Oak Ridge National Laboratory, Oak Ridge, TN 37831, USA

^dDepartments of Chemistry and Chemical and Biomolecular Engineering, University of Tennessee, Knoxville, TN 37996, USA

^eDepartment of Polymer Science and Engineering, Pusan National University, Busan 46241, Korea

Email: skahn@pusan.ac.kr and mkilbey@utk.edu

Experimental

1. Materials

The highly active, rapidly-initiating ruthenium based metathesis catalyst, $(\text{H}_2\text{IMes})(\text{pyr})_2(\text{Cl})_2\text{RuCHPh}$, was synthesized as previously described¹ and quickly used immediately after synthesis. All other reagents were used as received unless otherwise noted.

2. Materials Synthesis

Synthesis of macromonomers

Synthesis of norbornenyl-functionalized poly(3-hexylthiophene) (P3HT macromonomer, MM_{P3HT}) and norbornenyl-functionalized poly(D,L-lactide) (PLA macromonomer, MM_{PLA}) are described in detail in our previous publications.^{2,3} The molecular weights of the macromonomers, determined by end-group analysis using ^1H NMR spectroscopy, were 3.6 kDa for MM_{P3HT} containing ~5% impurity, and 4.0 kDa for MM_{P3HT} containing ~20% impurity and 5.3 kDa for MM_{PLA} .

Synthesis of random bottlebrush copolymers

In a representative experiment, the MM_{P3HT} (9.5 μmol) and the MM_{PLA} (7.55 μmol) were added to a clean, dry glass scintillation vial. The vial was then capped with a rubber septum. To this vial, 1.5 mL of dry chloroform was added and the headspace purged with nitrogen. In a separate vial, a stock solution (3.44 μmol , 0.344 mM) of $(\text{H}_2\text{IMes})(\text{pyr})_2(\text{Cl})_2\text{RuCHPh}$ in dry chloroform (10 mL) was prepared and purged with nitrogen. To start the polymerization, a portion of the catalyst solution (0.344 μmol , 1 mL) was transferred to the macromonomer solution, and the mixture was stirred for 90 min at room temperature. An excess amount of ethyl vinyl ether (EVE, 0.1 mL) was added to terminate the reaction. The reaction mixture was concentrated by rotary evaporation, precipitated into methanol and filtered. The precipitate was vacuum-dried overnight at room temperature.

Molecular weight of bottlebrush copolymers was measured by size exclusion chromatography (SEC) with light scattering detection using specific refractive index increment (dn/dc) of bottlebrush copolymers estimated from $[(dn/dc) \text{ of } \text{MM}_{\text{P3HT}} \times \text{mass fraction of}$

$MM_{P3HT}] + [(dn/dc) \text{ of } MM_{PLA} \times \text{mass fraction of } MM_{PLA}]$, where dn/dc of 0.3 and 0.05 mL/g in THF were used for MM_{P3HT} and MM_{PLA} , respectively.

	dn/dc of MM_{P3HT} (mL/g)	Mass fraction of P3HT	dn/dc of MM_{PLA} (mL/g)	Mass fraction of PLA	dn/dc of bottlebrush copolymer (mL/g)
R21 _{P3HT3.6k}	0.3	0.19	0.05	0.81	0.098
R46 _{P3HT3.6k}	0.3	0.43	0.05	0.57	0.158
R71 _{P3HT3.6k}	0.3	0.69	0.05	0.31	0.224
R29 _{P3HT4k}	0.3	0.27	0.05	0.73	0.118
R50 _{P3HT4k}	0.3	0.48	0.05	0.52	0.170
R73 _{P3HT4k}	0.3	0.72	0.05	0.28	0.229

3. Methods and Characterizations

¹H NMR spectroscopy was performed on Varian Unity 500 wide bore multinuclear spectrometer with deuterated chloroform as solvent. SEC was performed using an Agilent 1260 Infinity Binary pump equipped with Agilent 1200 Series PDA detector, a Wyatt Dawn Heleos II 18-angle laser light scattering detector and a Wyatt Optilab T-rEX refractometer. THF was used as eluent, and ASTRA 6.1 software was used to calculate molecular weight from light scattering. Differential scanning calorimetry (DSC) measurements were performed using TA instruments (Q1000) with a heat/cool/heat protocol under nitrogen flow. Samples (2-4 mg) were first heated to 250 °C to remove thermal history, then cooled to -100 °C, and re-heated to 250 °C using a ramp rate of 10 °C/min. The first cooling and the second heating cycles were used to determine transition temperatures. Attenuated total reflectance Fourier transform infrared spectroscopy (ATR-FTIR) spectra were obtained using a Harrick Scientific VariGATR accessory coupled with a Bruker Optics Vertex 70 spectrometer equipped with a narrow-band (650 cm⁻¹ cutoff), liquid nitrogen-cooled MCT detector. The bottlebrush copolymer films created by spin-casting on silicon substrates were placed on the ATR crystal and intimate contact obtained by applying 500 N of pressure. A background spectrum (128 scans at 4 cm⁻¹ resolution) of the clean ATR crystal was used as the reference spectrum. An aperture setting of 6 mm and a scanner velocity of 10 kHz were used. The Fourier transform parameters used are as follows: apodization function of Blackman-Harris 3-Term; phase resolution of 32 cm⁻¹; phase correction mode of Mertz; zero filling factor of 2. The acquisition parameters used were a mode of double-sided, forward-backward and 256 scans at a resolution of 4 cm⁻¹. A Woollam M-2000U variable angle

spectroscopic ellipsometer, which uses a white light source with a wavelength range of 245-999 nm, was used to determine the thickness of the bottlebrush copolymer films. Thicknesses reported are the average of measurements made from at least three spots on the polymer-modified wafer. To fit the ellipsometric data, the polymer layer was represented as a slab of uniform thickness and sharp interface having optical properties described by a Cauchy model (refractive index smoothly varying with wavelength) assuming that the bottlebrush polymer film had refractive index of 1.50 at 632 nm.

Synchrotron X-ray scattering

Simultaneous small- and wide-angle X-ray scattering measurements were performed on the DND-CAT 5ID-D beamline at the Advanced Photon Source (Argonne National Laboratory) using an incident beam of wavelength ($\lambda = 0.73 \text{ \AA}$). Each measurement was conducted at three different sample-to-detector distances (0.2, 1.0 and 7.5 m) to cover a q -range of $0.0026 < q \text{ (\AA}^{-1}\text{)} < 4.4$, where $q = (4\pi/\lambda) \sin(\theta/2)$ is the magnitude of the scattering vector, and θ is the scattering angle. For X-ray scattering experiments, samples having thickness of $\sim 250 \text{ }\mu\text{m}$ were prepared by hot-pressing powder materials using the Specac Mini-Film Maker at $80 \text{ }^\circ\text{C}$ under a nitrogen environment. Temperature-dependent measurements were enabled using a heating stage (Linkam THMS600) in which the samples were sandwiched between two Kapton® films. At each set temperature, measured by a thermocouple, the samples were allowed to equilibrate at least for 2 min before data acquisition.

Transmission electron microscopy

Transmission electron microscopy (TEM) images were obtained using a Zeiss Libra 120 transmission electron microscope. The samples after characterization by temperature-resolved synchrotron X-ray scattering were also used for TEM analyses. These samples were embedded in low viscosity epoxy (Ted Pella), and cured at $50 \text{ }^\circ\text{C}$ for overnight. Afterward, samples were microtomed using a diamond knife (Leica and Diatome) at ambient temperature producing thin film sections with thicknesses of $\sim 75 \text{ nm}$. The thin sections floated on water were placed onto carbon-coated grids and imaged without staining.

Surface morphology

Surface morphologies were investigated using a Bruker Dimension Icon atomic force microscope (AFM) operated in tapping mode. Silicon wafers were pre-cleaned by sonication in acetone and isopropanol, followed by plasma treatment for 30 min. Films were created by depositing 1 mL of a filtered toluene solution (1 wt%), followed by spinning at 1500 rpm for 30 seconds. Afterwards, the polymer coated substrates were thermally annealed at 150 °C under vacuum for 45 h.

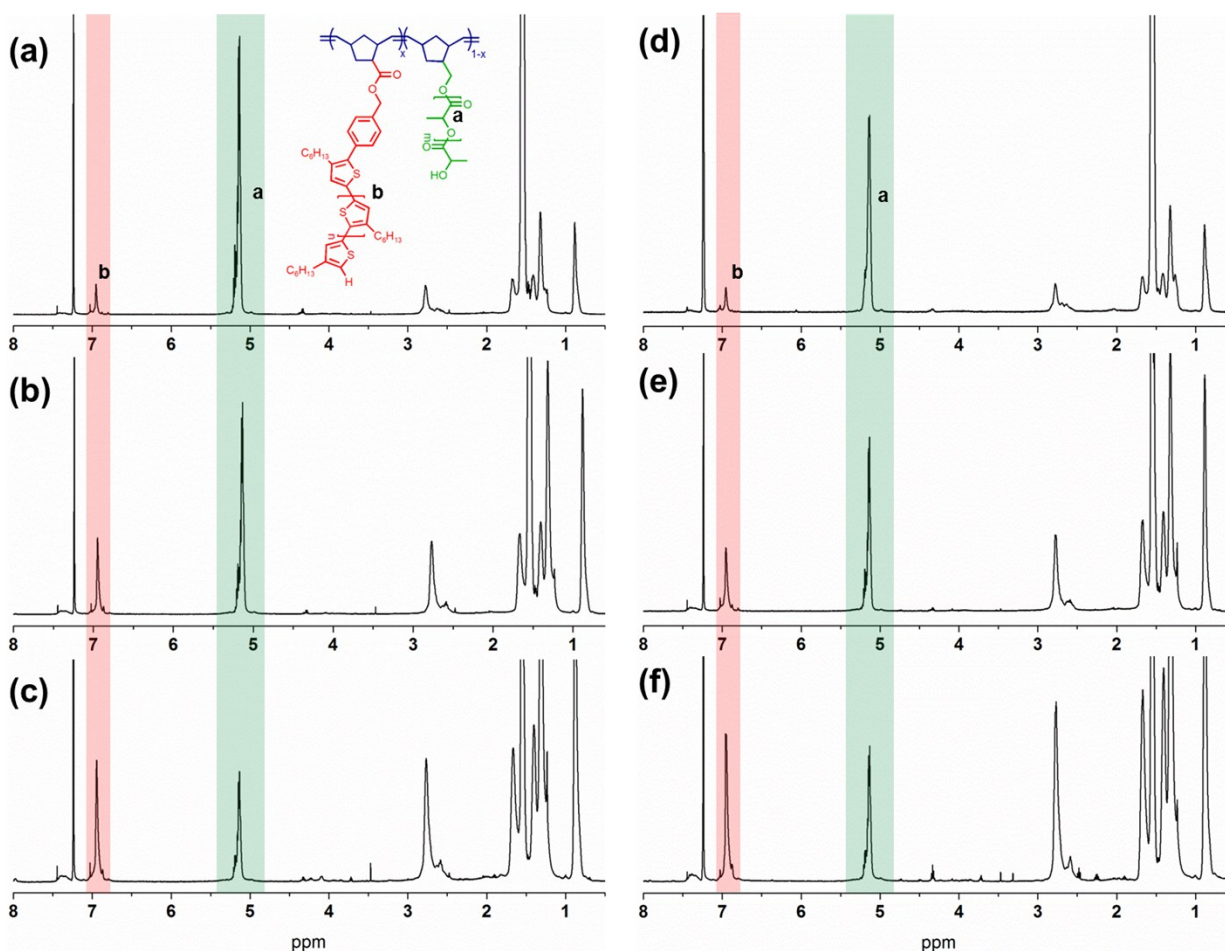


Figure S1. ^1H NMR spectra of random bottlebrush copolymers collected in CDCl_3 . (a) $\text{R21}_{\text{P3HT3.6k}}$, (b) $\text{R46}_{\text{P3HT3.6k}}$, (c) $\text{R71}_{\text{P3HT3.6k}}$, (d) $\text{R29}_{\text{P3HT4k}}$, (e) $\text{R50}_{\text{P3HT4k}}$ and (f) $\text{R73}_{\text{P3HT4k}}$. Integration values of the peak “a” for a proton in PLA and the peak “b” for a proton in P3HT are compared to determine relative composition of PLA and P3HT side chains.

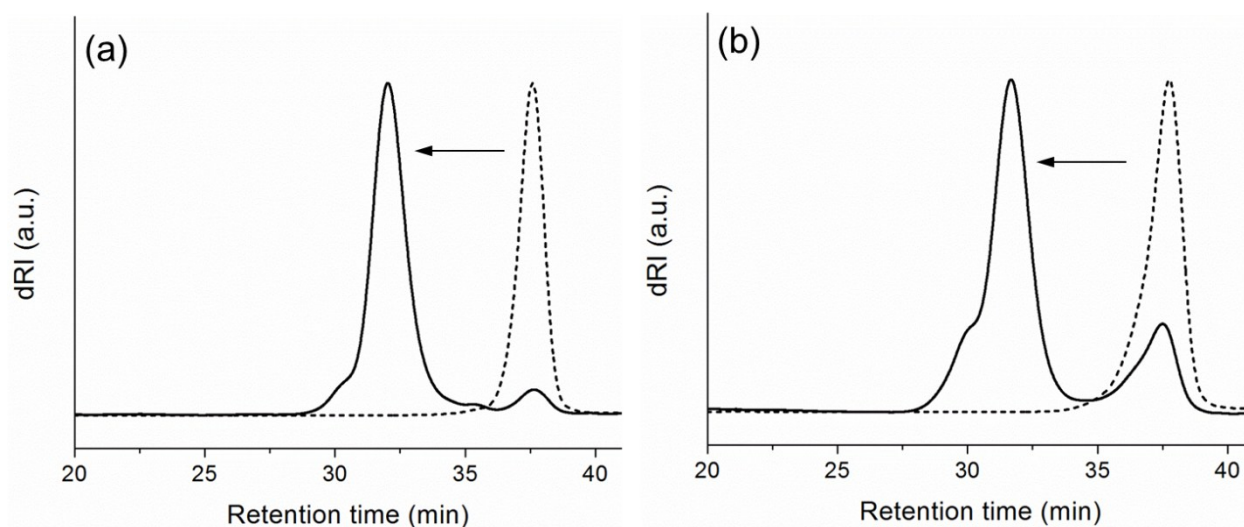


Figure S2. SEC traces of P3HT molecular bottlebrushes from a crude polymer solution prior to any drying process. (a) P3HT molecular bottlebrushes (solid) made from $MM_{P3HT3.6k}$ (short dash) containing about 5 wt% linear P3HT impurity and (b) P3HT molecular bottlebrushes (solid) made from MM_{P3HT4k} (short dash) containing about 20% linear P3HT impurity. Amount of P3HT impurity is estimated by comparing the peak area of bottlebrush to the peak area of residual macromonomer.

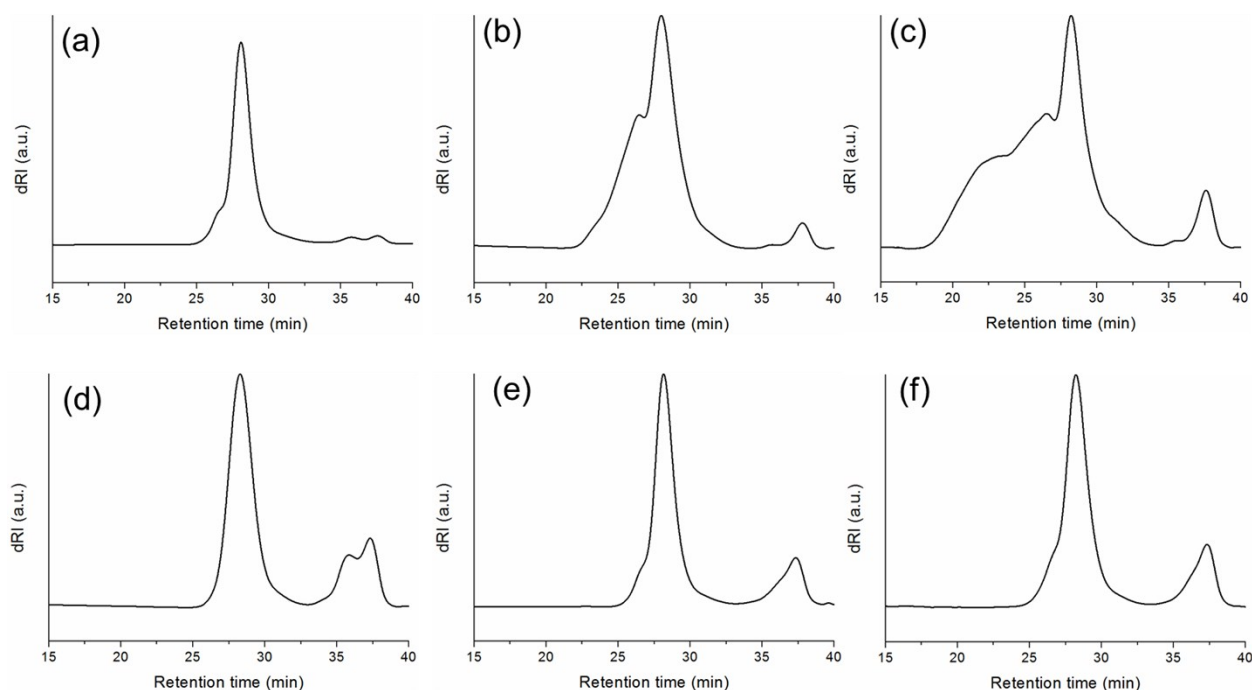


Figure S3. SEC traces of random bottlebrush copolymers after vacuum drying. (a) $R21_{P3HT3.6k}$, (b) $R46_{P3HT3.6k}$, (c) $R71_{P3HT3.6k}$, (d) $R29_{P3HT4k}$, (e) $R50_{P3HT4k}$ and (f) $R73_{P3HT4k}$.

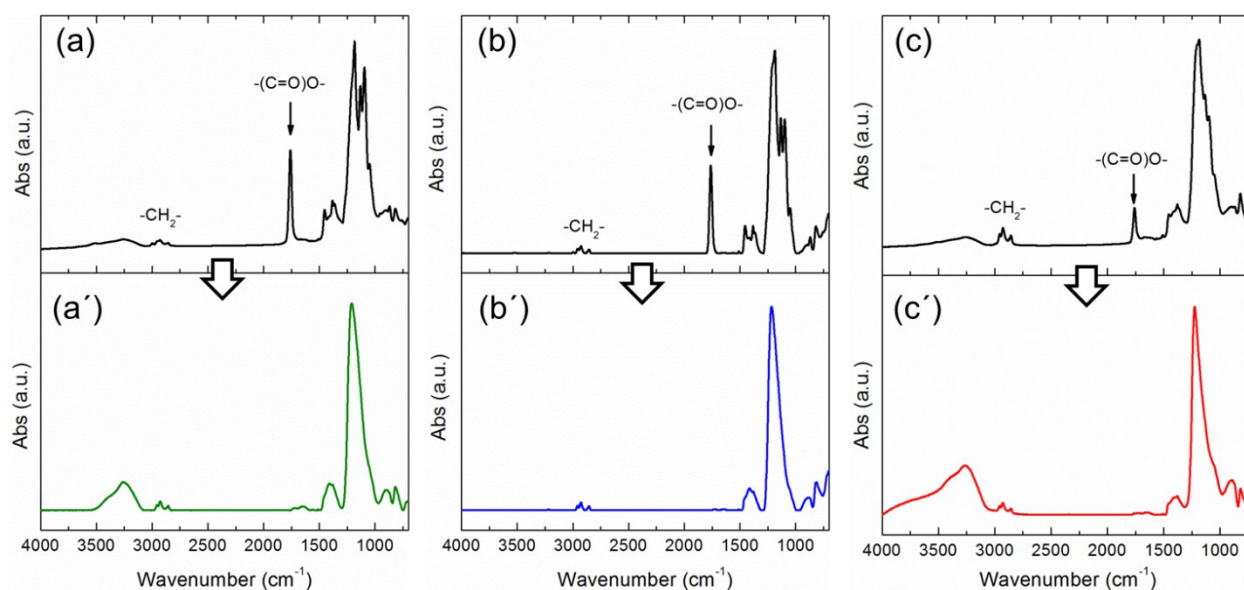


Figure S4. ATR-FTIR spectra of random bottlebrush copolymers before (top) and after (bottom) hydrolysis. (a and a') R29_{P3HT4k}, (b and b') R50_{P3HT4k} and (c and c') R73_{P3HT4k}.

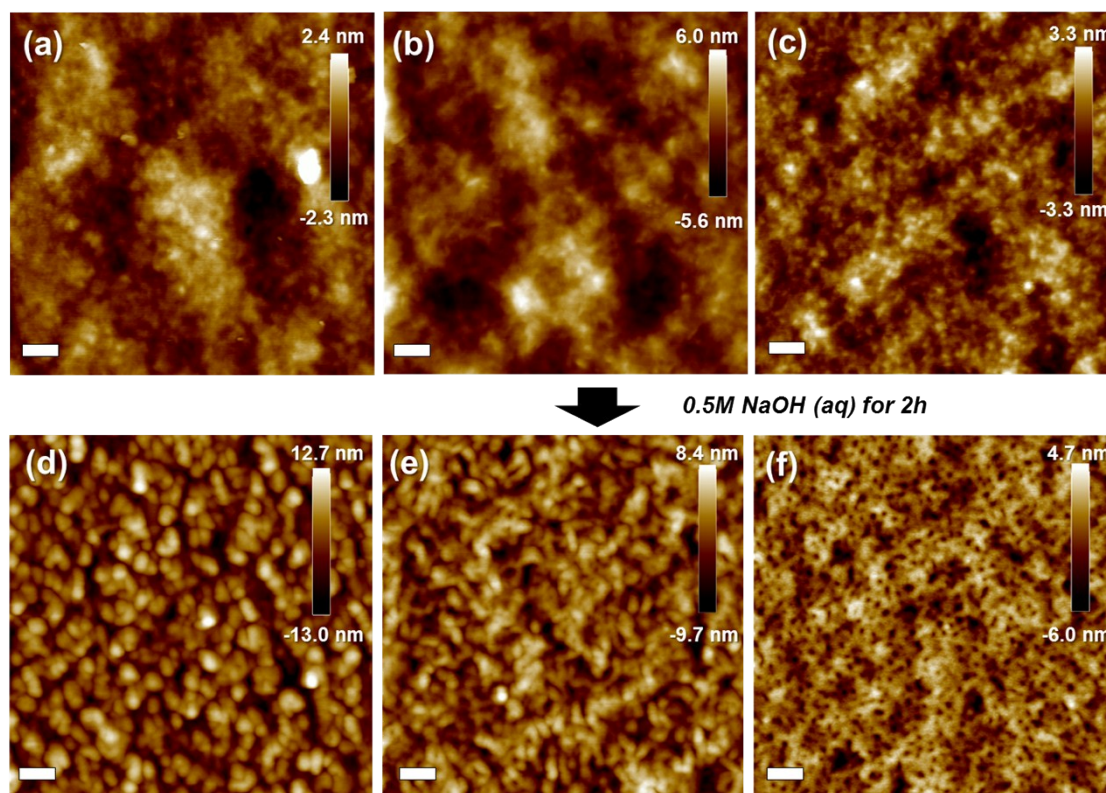


Figure S5. Representative tapping mode AFM height images of random bottlebrush copolymers: (top row) thermally-annealed samples and (bottom row) thermally-annealed followed by hydrolysis in NaOH (0.5M) for 2 h (Scale bars: 100 nm). (a and d) R29_{P3HT4k}, (b and e) R50_{P3HT4k} and (c and f) R73_{P3HT4k}.

Simulation Details

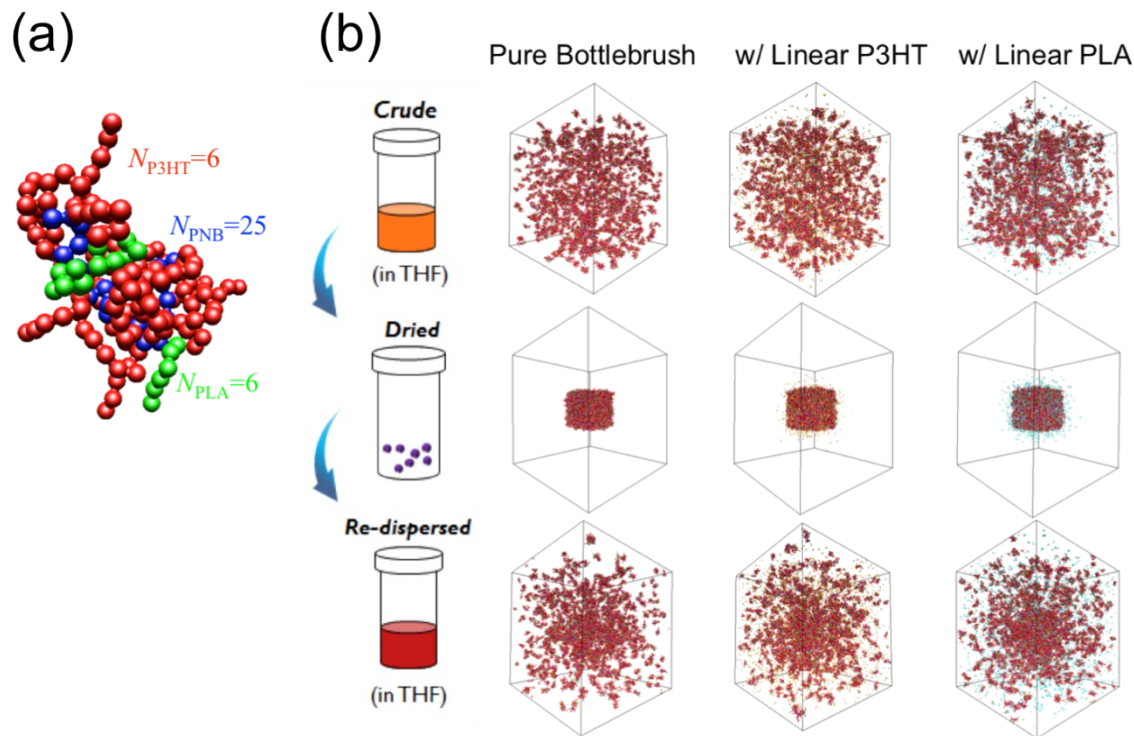


Figure S6. (a) Bottlebrush configuration showing the polynorbornene (PNB) backbone beads (blue), P3HT side chain beads (red) and PLA side chain beads (green). (b) Drying and dissolution processes for bottlebrushes without and with addition of linear P3HT (orange) or PLA (cyan) chains and $\phi = 88$.

Our previous coarse-grained molecular dynamics simulation of bottlebrushes² undergoing drying and dissolution was extended to include moieties of PLA. The structure of the bottlebrush is shown in Figure S6(a), where red, green and blue beads represent moieties of P3HT, PLA and PNB, respectively. Also we simulated two more systems that are composed of a mixture of bottlebrushes and linear P3HT (orange beads) or PLA (cyan beads). (see Figure S6(b)) The PNB backbone of the bottlebrush macromolecule is composed of $N_{\text{PNB}} = 25$ Lennard-Jones beads. Each backbone bead is grafted with a side chain composed of either P3HT or PLA side chains with six connected beads ($N_{\text{P3HT}} = N_{\text{PLA}} = 6$). The diameter of every bead is equal to σ . The composition of the number of P3HT side chains relative to PLA side chains is determined by $\phi = \text{MM}_{\text{P3HT}} / (\text{MM}_{\text{P3HT}} + \text{MM}_{\text{PLA}})$ where MM_{P3HT} and MM_{PLA} are the number of P3HT or PLA

grafted side chains, respectively. We simulated systems having different values of $\phi = \{0.0, 0.28, 0.52, 0.76, 0.88, 1.0\}$.

Every bond in the macromolecule (bottlebrush and linear chains) was described by the finite extensible nonlinear elastic (FENE) bond. The attractive portion of the FENE potential is described by,

$$U_{FENE}(r) = -0.5k_s R_m^2 \ln\left(1 - \frac{r^2}{R_m^2}\right), \quad (\text{S.1})$$

where $k_s = 30.0 k_B T / \sigma^2$, $R_m = 1.5 \sigma$, k_B is the Boltzmann constant and T is the absolute temperature. The repulsive interaction between two connected beads is described by the WCA potential with $\varepsilon_{LJ} = 1.5 k_B T$;

$$U_{WCA}(r) = \begin{cases} 4\varepsilon_{LJ} \left[\left(\frac{\sigma}{r} \right)^{12} - \left(\frac{\sigma}{r} \right)^6 \right] + \varepsilon_{LJ} & r < 2^{1/6} \sigma \\ 0 & r \geq 2^{1/6} \sigma \end{cases}. \quad (\text{S.2})$$

The backbone beads interact with other beads through the WCA potential (purely repulsive) with $\varepsilon_{LJ} = 1.0 k_B T$. The side chain-to-side chain, side chain-to-linear chain, and linear chain-to-linear chain interactions are described by a truncated and shifted Lennard-Jones potential,

$$U_{LJ}(r) = \begin{cases} 4\varepsilon_{LJ} \left[\left(\frac{\sigma}{r} \right)^{12} - \left(\frac{\sigma}{r} \right)^6 - \left(\frac{\sigma}{r_{\text{cut}}} \right)^{12} + \left(\frac{\sigma}{r_{\text{cut}}} \right)^6 \right] & r \leq r_{\text{cut}} \\ 0 & r > r_{\text{cut}} \end{cases}, \quad (\text{S.3})$$

with well depth ε_{LJ} and r_{cut} parameters listed in Table S1.

Table S1. Lennard-Jones interaction parameters used in the simulations.

	$\varepsilon_{\text{LJ}} (k_B T)$	$r_{\text{cut}} (\sigma)$
PNB-PNB	1.000	$2^{1/6}$
PNB-P3HT	1.000	$2^{1/6}$
PNB-PLA	1.000	$2^{1/6}$
P3HT-P3HT	0.430	2.5
P3HT-PLA	0.328 ^a	2.5
PLA-PLA	0.250	2.5

$$^a \varepsilon_{P3HT-PLA} = (\varepsilon_{P3HT-P3HT} \times \varepsilon_{PLA-PLA})^{1/2}$$

An angle potential,

$$U_{i,i+1}^{bend} = k_B T K_{\text{bend}} \left(1 - (\hat{n}_i \cdot \hat{n}_{i+1}) \right) \quad (\text{S.4})$$

is included in the P3HT side chains and P3HT linear chains to promote chain rigidity. The parameters in eq. S.4. is $K_{\text{bend}} = 3.0$ for polymer unit bond vectors \hat{n}_i and \hat{n}_{i+1} . In this case, the persistence length of P3HT is $\sim 3\sigma$.

Simulations were carried out in the canonical ensemble (NVT) with implicit solvent. The temperature was maintained by coupling the system to a Langevin thermostat with friction coefficient, ζ , set to $m/(7\tau)$ where τ is the reduced time unit. In this case, the equation of motion of the i^{th} bead is

$$m \frac{d\hat{v}_i(t)}{dt} = \hat{F}_i(t) - \zeta \hat{v}_i(t) + \hat{F}_i^R(t), \quad (\text{S.5})$$

where $\hat{v}_i(t)$ is the i^{th} bead velocity and $\hat{F}_i(t)$ is the net deterministic force acting on the bead with mass, m . $\hat{F}_i^R(t)$ is the stochastic force with zero average value $\langle \hat{F}_i^R(t) \rangle = 0$ and δ -functional

correlations $\langle \overset{\text{U}}{F}_i^R(t) \overset{\text{U}}{F}_i^R(t') \rangle = 6\xi k_B T \delta(t - t')$. The velocity-Verlet algorithm with a time step of 0.01 τ was used for time integration.

To simulate the drying and dissolution processes, 1000 bottlebrushes were initially arranged in a $10 \times 10 \times 10$ cubic lattice with an initial side chain monomer density of $0.01 \sigma^{-3}$ and were ran up to $2 \times 10^4 \tau_{LJ}$. Drying was modeled by increasing the side chain monomer density to $0.3 \sigma^{-3}$ to promote inter-brush contact. The drying stage was ran up to $10^3 \tau_{LJ}$ after which the side chain monomer density was decreased back to $0.01 \sigma^{-3}$ to model the dissolution of the aggregated bottlebrushes. The dissolution step was run up to $10^5 \tau_{LJ}$. These steps are shown in Figure S6(b). To model the effect of addition of short linear P3HT or PLA chains on the extent of aggregation of bottlebrushes after the drying and dissolution processes, the same simulation protocol was repeated, but with the addition of 2500 linear P3HT or PLA chains for the system with $\phi = 88$.

References

- (1) Love, J. A.; Morgan, J. P.; Trnka, T. M.; Grubbs, R. H. *Angew. Chem. Int. Ed.* **2002**, *41*, 4035-4037.
- (2) S.-k. Ahn, D. L. Pickel, W. M. Kochemba, J. Chen, D. Uhrig, J. P. Hinestrosa, J.-M. Carrillo, M. Shao, C. Do, J. M. Messman, W. M. Brown, B. G. Sumpter, S. M. Kilbey II, *ACS Macro Lett.*, **2013**, *2*, 761-765.
- (3) S.-k. Ahn, J.-M. Y. Carrillo, Y. Han, T.-H. Kim, D. Uhrig, D. L. Pickel, K. Hong, S. M. Kilbey, B. G. Sumpter, G. S. Smith, C. Do, *ACS Macro Lett.*, **2014**, *3*, 862-866.